

Evidence of phonon mediated coupling between charge transfer and ligand field excitons in $\text{Sr}_2\text{CuO}_2\text{Cl}_2$

R. Lövenich, A. B. Schumacher[†], J. S. Dodge[‡], and D. S. Chemla

Department of Physics, University of California at Berkeley, Berkeley, California 94720

*Materials Sciences Division, E. O. Lawrence Berkeley National Laboratory, Berkeley, California
94720*

L. L. Miller

Ames Laboratory and Department of Physics, Iowa State University, Ames, IA 50011

(November 1, 2018)

Abstract

We present a comparative experimental and theoretical investigation of the two-dimensional charge-transfer gap in the strongly correlated material $\text{Sr}_2\text{CuO}_2\text{Cl}_2$. We observe an Urbach behaviour in the absorption profile over a surprisingly wide range of energies and temperatures. We present a model that accounts for phonon scattering to infinite order and which allows us to explain the data accurately by assuming coupling of the charge transfer gap exciton to lower energy electronic excitations.

I. INTRODUCTION

The excitation spectrum of transition metal oxides is characterized by strong coupling of spin, charge, orbital and lattice degrees of freedom, and the complexity of these interactions has severely hindered progress in understanding the phenomenon of high-temperature superconductivity in the layered copper oxides. Even the basic energy level spectrum of the undoped, insulating cuprates continues to be controversial. The dominant optical absorption feature in these materials is a broad excitonic peak at the charge-transfer (CT) gap, about half an electron volt wide, which exhibits strong dependence on temperature and doping^{1,2}. Despite the strong interest in insulating cuprates and the fundamental physical significance of the CT gap exciton, few attempts have been made to explain its structure and coupling to phonons^{2,3}.

In this paper, we present an experimental investigation of the linear absorption of $\text{Sr}_2\text{CuO}_2\text{Cl}_2$ and a new theory for the CT excitation in the CuO-plane. The theory includes the coupling of the exciton to phonons and to an additional, low energy electronic continuum of states. It explains the linear absorption of $\text{Sr}_2\text{CuO}_2\text{Cl}_2$, and in particular the Urbach behaviour over a wide range of temperatures and energies.

II. SAMPLE STRUCTURE

$\text{Sr}_2\text{CuO}_2\text{Cl}_2$ is a two-dimensional, spin-1/2 Heisenberg antiferromagnet with a Néel temperature $T_N \approx 250$ K and an exchange interaction energy $J=125$ meV⁴. In the ground state a single hole per CuO_2 unit cell is located on the Cu site and exhibits a $3d_{x^2-y^2}$ symmetry.

The lowest energy optically allowed electronic excitation in this material corresponds to the Cu $3d_{x^2-y^2}$ to O $2p\sigma$ transfer of a hole in the CuO_2 layer. This transition classifies the material as a charge-transfer insulator⁵. The optical absorption spectrum consists mainly of a rather sharp peak near the band edge at about 2 eV and another wider peak at about 2.5 eV⁶. A detailed analysis of the energy region below the band edge reveals a weak ab-

sorption step at about 1.4 eV, two orders of magnitude smaller than the main CT structure. It is attributed to a Cu ligand field transition⁷, which should be optically forbidden, but acquires a small oscillator strength owing to a breaking of the crystal symmetry. This transition has also been observed in resonant X-ray Raman spectroscopy⁸ and large-shift Raman scattering⁹.

The dominant peak at the band edge is attributed to a bound excitonic state. A model by Zhang and Ng³ predicts an exciton formed by an electron at a Cu site and a delocalized hole at the four neighbouring O sites, with a stronger weight at the O site from which the electron came. The model gives a large bandwidth for the center of mass motion of this exciton of about 1.5 eV¹⁰. This means that the exciton has an effective mass smaller than the electron or hole alone, which can be understood by the fact that the transfer of the exciton from one site to another does not disturb the antiferromagnetic order of the background.

III. EXPERIMENT

We used high quality single crystals of Sr₂CuO₂Cl₂ which were grown by the technique described in Ref. 11. This method yields platelets with a fairly large (001) surface. By tape-cleaving the crystals, we reduced the sample thickness, d , to below 100 nm. These thin samples enabled us to measure the absorption coefficient, $\alpha(\omega)$, across the charge transfer gap directly, by comparing as a function the frequency ω the intensity transmitted through the sample on the substrate, I_{Tot} , with the intensity transmitted through the substrate only, I_{Sub} : $\alpha(\omega) = -\frac{1}{d} \ln(\frac{I_{Tot}}{I_{Sub}})$. This procedure is more precise and direct than the previous reflectivity measurements, which relied on Kramers-Kronig transformation to extract information about the absorption coefficient¹². Figure 1 shows the linear absorption coefficient for selected temperatures. The crystal used for this measurement was $d = 95 \pm 5$ nm thick and held inside a cold finger cryostat. The inset details the weak onset of the absorption at 1.4 eV and was measured using a 300 μ m thick sample.

The excitonic peak shows a strong temperature dependence. With increasing tempera-

ture the width — measured as the half width at half maximum — increases from 180 meV at 15 K to 270 meV at 350 K. The maximum exhibits a redshift of about 80 meV in this temperature range. The temperature dependence of the excitonic peak is shown in figure 2. Both the shift towards lower energies and the broadening can be fit by a Bose–Einstein occupation function with a single oscillator². From this fit we find the energy of this oscillator, $\hbar\omega_0 \approx 45$ meV, to agree with that of a previously identified bond–bending longitudinal optical (LO) phonon¹³ and well below the characteristic magnetic energy of $J=125$ meV in $\text{Sr}_2\text{CuO}_2\text{Cl}_2$. Experimental evidence therefore suggests coupling of the CT-exciton to phonons rather than to magnetic excitations as the origin of its red shift and broadening². This is further supported by a careful analysis of the line shape of the low energy side of the CT excitation. As shown in figure 3, $\alpha(\omega)$ exhibits an exponential behaviour over a wide range of temperatures and energies. We find the experimental data can be fit very well to the Urbach formula

$$\alpha(\omega, T) = \alpha_0 \exp \frac{\sigma(T)(E - E_0)}{k_B T}; \quad (1)$$

$$\sigma(T) = \sigma_0 \frac{2k_B T}{\hbar\omega_0} \tanh \frac{\hbar\omega_0}{2k_B T}. \quad (2)$$

where E_0 and α_0 are temperature independent parameters, and $\hbar\omega_0$ is the energy of the phonon to which the exciton couples. The parameter σ_0 yields information on the strength of this coupling and E_0 is related to the strength of the exciton binding. From a global best fit to the data plotted in figure 3 data we obtain $\hbar\omega_0=45$ meV, $E_0=1.95$ eV and $\sigma_0 = 0.35$. The latter indicates a very strong coupling between excitons and phonons. Furthermore, the fact that E_0 is smaller than the energy $E(\alpha=\text{max})$ where the absorption is maximal, suggests a tightly bound exciton¹⁴.

It is worth noting that it is very surprising to observe an Urbach behavior at temperature as low as 15 K where the occupation probability of LO–phonons with $\hbar\omega_0=45$ meV is $N_0 \approx 2 \times 10^{-16}$ and absorption of thermal phonons is negligible.

IV. THEORY

To the best of our knowledge, the model of Falck et al.² is the only one in the literature describing the temperature dependence of the CT excitations. Falck et al.² investigated the absorption line shape of a related compound, the charge–transfer insulator La_2CuO_4 . The excitonic peak in this material also shows a temperature shift and broadening. Approximating the Coulomb interaction with an attractive contact interaction between the electron and hole, they derived a simple expression for the absorption coefficient. While without interactions the interband contribution to the absorption is just the density of states, the Coulomb interaction leads to an increase of the absorption near the band edge. This describes the basic shape of the spectrum. Falck et al. account for the shift of the band edge and the finite lifetime of the exciton by inserting the real and imaginary part of the one–phonon self energy. With four parameters they are able to fit well the linear absorption in La_2CuO_4 .

Our experimental results show the exponential behavior of an Urbach tail down to very low temperatures. It is in striking contradiction with the prediction of Ref. 2, which by construction always produces a Lorentzian tail. The coupling constant used in Ref. 2 was $\alpha = 10.8^{15}$. This is an extremely high value compared to normal semiconductors (where it is well below 1.0) and even other materials with a strong electron–phonon coupling. For such a high coupling constant the one–phonon approximation is no longer valid.

Since a strong coupling to LO–phonons seems to be the reason for the strong temperature dependence of the spectra, we propose a more advanced model, taking into account many–phonon processes. The approach was inspired by results obtained for conventional semiconductors¹⁶, where Urbach tails are found for high temperatures.

The theoretical analysis is organized as follows: First we introduce the Hamiltonian in an exciton basis. The Green’s function of that Hamiltonian will be calculated by means of the cumulant expansion. We will then discuss the dependence of the results on model parameters for different cases of physical interest. We will show that it is necessary to include ligand field (LF) excitations, which were not yet known at the time of Ref.². These

are the states into which the CT exciton can scatter even at low temperatures by phonon emission, thus leading to the Urbach tail.

The model Hamiltonian:

$$H = H_0 + V \quad (3)$$

$$H_0 = \sum_{jn\mathbf{k}} E_{n,\mathbf{k}}^j a_{n,\mathbf{k}}^{j\dagger} a_{n,\mathbf{k}}^j + \hbar\omega_0 \sum_{\mathbf{q}} b_{\mathbf{q}}^\dagger b_{\mathbf{q}} \quad (4)$$

$$V = \sum_{jj'} \sum_{nm\mathbf{q}} M_{nm,\mathbf{q}}^{jj'} a_{n,\mathbf{k}+\mathbf{q}}^{j\dagger} a_{m,\mathbf{k}}^{j'} [b_{\mathbf{q}} + b_{-\mathbf{q}}^\dagger] \quad (5)$$

is written in an exciton basis, where $a_{n,\mathbf{k}}^{j\dagger}$ is the creation operator for an exciton of type j , internal quantum number n and center of mass momentum \mathbf{k} . In the case of the j =CT exciton we account for a bound state ($n = 0$), and for the unbound exciton electron–hole continuum ($n > 0$). The pair (n, \mathbf{k}) can then be transformed to the pair of electron and hole momentum, which is more suited to describe the free electron–hole pair. In the case of the ligand field excitation (j =LF) we consider continuum states only. The operators $b_{\mathbf{q}}$ and $b_{\mathbf{q}}^\dagger$ respectively describe the annihilation and creation of an dispersionless LO–phonon of frequency ω_0 .

The imaginary part of the dielectric function and hence the spectral features of the absorption coefficient are given by the imaginary part of the retarded Green’s function

$$\varepsilon_2(\omega) \propto \text{Im} \left\{ \sum_{j=\text{CT}, n\mathbf{k}} G^j(n\mathbf{k} = 0; \omega) \right\}, \quad (6)$$

where the summation includes only the optically active CT–exciton.

Since the excitation starts from a ground state characterized by empty hole and electron states, the retarded Green’s function equals the time–ordered one, for which an expansion in the electron–phonon coupling exists:

$$G^j(n\mathbf{k}; t) = -\frac{i}{\hbar} \theta(t) \sum_{\nu=0}^{\infty} W_{\nu}^j(n\mathbf{k}; t) \quad (7)$$

$$W_{\nu}^j(n\mathbf{k}; t) = \frac{(-i)^{2\nu}}{\hbar^{2\nu} (2\nu)!} \int_0^t dt_1 \dots \int_0^t dt_{2\nu} \langle T \bar{a}_{n,\mathbf{k}}^j(t) \bar{V}(t_1) \dots \bar{V}(t_{2\nu}) \bar{a}_{n,\mathbf{k}}^{j\dagger}(0) \rangle, \quad (8)$$

with the time-ordering operator T . The unperturbed Green's function is given by $G_0^j(n\mathbf{k}; t) = -i/\hbar \theta(t) \exp(-iE_{n,\mathbf{k}}^j t/\hbar)$. The first order term in (7) would give rise to one-phonon processes. However, it is possible to account for multi-phonon processes by resumming the expansion Eq. (7) in form of an exponential, leading to the cumulant expansion or linked-cluster theory. We write

$$G^j(n\mathbf{k}; t) = G_0^j(n\mathbf{k}; t) \exp\left(\sum_{\nu=1}^{\infty} F_{\nu}^j(n\mathbf{k}; t)\right), \quad (9)$$

where F_{ν} denotes a contribution which contains the 2ν -th power of the coupling matrix-element. Comparing the different powers of the expansions (7) and (9) the following relations hold:

$$F_1^j(n\mathbf{k}; t) = e^{iE_{n,\mathbf{k}}^j t/\hbar} W_1^j(n\mathbf{k}; t) \quad (10)$$

$$F_2^j(n\mathbf{k}; t) = e^{iE_{n,\mathbf{k}}^j t/\hbar} W_2^j(n\mathbf{k}; t) - \frac{1}{2!} F_1^{j2}(n\mathbf{k}; t). \quad (11)$$

The advantage of this re-summation is that F_1 already includes independent phonon scattering to infinite order. Thus as long as they are independent from each other, the first term in the cumulant expansion F_1 accounts for all these contributions in contrast to the expansion (7). Similarly F_2 describes all electron-phonon interactions involving simultaneously two phonons, etc. The cumulant expansion (9) is expected to converge much faster than (7) and to be appropriate for low and intermediate coupling constants. Up to now we restricted ourself to the lowest order only, which means that we treat the fields induced by the lattice distortions classically.

The time-integrations in (8) can be performed analytically, yielding:

$$F_1^j(n\mathbf{k} = 0; t) = \sum_{h'm\mathbf{q}} \left| M_{nm,\mathbf{q}}^{jj'} \right|^2 \left\{ (N_0 + 1) \bar{f}(E_{m,\mathbf{q}}^{j'} - E_{n,0}^j + \hbar\omega_0, t) + N_0 \bar{f}(E_{m,\mathbf{q}}^{j'} - E_{n,0}^j - \hbar\omega_0, t) \right\}. \quad (12)$$

The time dependence is described by the function

$$\bar{f}(\varepsilon, t) = \frac{1}{\varepsilon^2} \left(1 - e^{-i\varepsilon t/\hbar} - \frac{i\varepsilon t}{\hbar} \right). \quad (13)$$

This function is regular for all values of ε and has its maximum value at $\varepsilon = 0$ for finite times, which in Eq. (12) corresponds to $E_{m,\mathbf{q}}^{j'} = E_{n,0}^j \pm \hbar\omega_0$, i.e. the absorption and emission of LO-phonons in the $(j', m\mathbf{q}) \leftrightarrow (j, n)$ transition. At low temperatures only the emission term proportional $(N_0 + 1) \rightarrow 1$ contributes, which peaks out one phonon energy below the CT exciton.

In order to keep our model simple, we neglect the \mathbf{q} dependence of the coupling matrix elements $M_{nm,\mathbf{q}}^{jj'}$ as well as the dependence on the relative momentum if $m > 0$ or $n > 0$, i.e., for the electron–hole continuum. This means we have to consider the following five scattering processes:

M_{xx} Scattering from the CT-exciton into its center of mass continuum;

M_{xc} Scattering from the CT-exciton into its own electron–hole continuum;

M_{cc} Scattering within the CT electron–hole continuum;

M_{xd} Scattering from the CT-exciton into the LF exciton band;

M_{cd} Scattering from the CT electron–hole continuum into the LF exciton band;

Since the matrix–elements do not depend on momentum variables any more, the summations over momentum variables in (12) can be transformed into energy integrals with the density of states into which the CT-exciton is scattered:

$$F_1(n = \{x, c\}, 0; t) = \int d\varepsilon \sum_{m=\{x,c,d\}} M_{nm} z_m(\varepsilon) \times \left\{ (N_0 + 1) \bar{f}(\varepsilon - E_{n,0} + \hbar\omega_0, t) + N_0 \bar{f}(\varepsilon - E_{n,0} - \hbar\omega_0, t) \right\}. \quad (14)$$

The densities of states are defined as:

$$z_x(\varepsilon) = \frac{1}{N} \sum_{\mathbf{q}} \delta(\varepsilon - E_{x,\mathbf{q}}) \quad \text{and} \quad (15)$$

$$z_c(\varepsilon) = \frac{1}{N^2} \sum_{\mathbf{qk}} \delta(\varepsilon - E_{\mathbf{k},\mathbf{q}}). \quad (16)$$

We model the energy dispersion of the exciton by a two dimensional tight binding dispersion $E_{x,\mathbf{q}} = B/4 \cdot (2 - \cos q_x - \cos q_y)$ with a bandwidth of $B=1.2$ eV and a electron-hole relative motion continuum, also with a 2d tight binding dispersion, but a 0.6 eV bandwidth. We have solved numerically Eq. (6) with this dispersion law in three cases of physical interest. In case (1) we consider the situation where phonon scattering occurs only within the CT-exciton states, i.e., CT bound-exciton and its electron-hole continuum, and the transitions into other exciton bands are not allowed, $M_{xd} = 0$ and $M_{cd} = 0$. In the other cases we assume that phonon scattering can also occur with other excitonic states^{17,9} (LF exciton band) of energy lower than the CT exciton, $M_{xd} \neq 0$ and $M_{cd} \neq 0$, and to explore the generality of our assumptions we consider two slightly different LF exciton bandwidths in the cases (2a) and (2b).

The results in case (1), for the contribution of the bound CT-exciton ($n = x$ in (9)) to the absorption only, are shown in figure 4 and are in obvious contradiction with experiment. Clearly the coupling to LO-phonons leads to a broadening of the CT-exciton line. It becomes asymmetric with a longer tail at the high energy side. On the low energy side, the spectrum has an Urbach tail, but the width is extremely small, especially at low temperatures. This is true even for very high coupling constants. Accounting for the large width at low temperatures by assuming an homogenous or inhomogenous broadening would lead to a Lorentzian or Gaussian profile of the lower energy side of the spectrum.

The shortcoming of our model in case (1) is clear. Since the Urbach behavior is observed at very low temperature phonon emission governs the interaction with the lattice as implied by Eq. (14). Therefore, for broad CT-exciton peak with a flat exponential tail to occur there must be states available below its energy and the CT-exciton must be able to couple to these states by phonons. Only then can LO-phonon scattering be strong even at zero temperature. Both our own data and the experiments in Ref. 6 show that such a continuum exists and starts at about 1.4 eV. It is assigned to Cu d-d transitions and can couple to the excitons by means of LO-phonons.

Therefore we expanded the model by including the continuum of LF excitations. Since

little is known about the bandwidth of these excitations^{17,9} we have considered two values for this parameter. In case (2a) we assumed that the LF bandwidth is the same as that of the CT electron–hole continuum. The CT exciton binding energy was fitted to be 240 meV, and $|M_{nm}|^2 = 20(\hbar\omega_0)^2$ was used for all the coupling constants. In addition to the LO–phonon broadening we included an inhomogeneous broadening $\Gamma_I=60$ meV to account for sample imperfections. An homogenous broadening also should be included, however, it must be very small compared to Γ_I because otherwise a Lorentzian profile would show up for energies far below the CT exciton energy in contradiction with experiment. Therefore, in order to limit the number of parameters we have not included it in our calculations. Finally, to fit the spectral contribution of the CT continuum we found that the spectral weight of the electron–hole continuum needs to be twice that of the exciton.

The solid lines in figures 5 and 6 show the theoretical results in case (2a) both on a linear and logarithmic scale. They are in excellent agreement with the experimental data, shown by the dots. The broadening and the shift of the CT exciton are reproduced correctly and even the decrease in oscillator strength is well described.

It may be argued that the LF excitations bandwidth should be smaller than that of the CT electron–hole continuum. In order to investigate this eventuality, we have considered in case (2b) the effects of a narrower LF bandwidth, only 1 eV, while maintaining the flat density of states starting at 1.4 eV in agreement with the experimental absorption spectrum. In that case we find that we can also achieve an excellent agreement with experiment, of the same quality as in case (2a) (not shown), but then we need two independent coupling constants, one describing the phonon coupling to the LF excitations and another coupling within the CT manifold. Interestingly, the numerical integration points out that the temperature shift of the CT exciton is governed by the coupling to its own continuum, whereas its broadening is mostly determined by the coupling to the LF excitations. With these two parameters the model is also robust against changes of the onset of the LF excitations.

Although the model formally has a number of fit parameters, many (phonon energy, CT exciton bandwidths, onset of LF excitations etc.) are fixed by experiment. Furthermore, we

have limited the number of parameters by limiting the number of phonon coupling constants to one (case-2a) or two (case-2b), so that in fact only few parameters are free: the (one or two) phonon coupling constants, the inhomogenous broadening, the relative spectral weight of the CT exciton and its continuum, the CT exciton binding energy and an overall scaling factor.

The results indicate that the coupling constants thus obtained are indeed large. Due to the different models they cannot be directly compared to the results of Falck et al. It is straight forward to check if accounting only for independent one-phonon processes is sufficient, since one can calculate F_2 with not too much effort if the \mathbf{q} -dependence of the matrix elements is neglected. This has not yet been done. Another theory often used to describe localized electronic excitations coupled to LO-phonons is Toyozawa's¹⁸. In the strong coupling regime it predicts a self-trapping of the excitons, i. e. due to the phonon cloud surrounding the exciton its effective mass becomes extremely large. Since we have shown on very general physical grounds that the low temperature Urbach behavior requires the coupling of the CT-exciton to a continuum of states below the exciton energy, we expect that a model based on Toyozawa's theory would give results qualitatively similar to ours.

In conclusion we have presented measurements of the linear absorption of the material $\text{Sr}_2\text{CuO}_2\text{Cl}_2$ which exhibits broadening and shift of the charge transfer gap exciton and, importantly, an Urbach behavior down to very low temperatures. This behavior cannot be explained by the current theories. We have developed a model based on a cumulant expansion that explains well all our data providing that the charge transfer gap exciton is coupled by LO-phonons to a continuum of states with lower energy. We identify this continuum with the Cu d-d continuum which is revealed in the linear absorption spectra owing to a weak crystal field symmetry breaking. A consequence of our interpretation is that the magnetic degrees of freedom do not seem to play a significant role in the temperature dependence of the charge transfer absorption edge in this material.

V. ACKNOWLEDGMENTS

The authors thank W. Schäfer, S. Louie and A. Millis for helpful comments. A. B. S. gratefully acknowledges support by the German National Merit Foundation. The work at Berkeley was supported by the Director, Office of Science, Office of Basic Energy Science, Division of Materials Sciences and Office of Science, U. S. Department of Energy under Contract No. DE-AC03-76SF00098. The work at Ames Laboratory was supported in part by the DOE Office of Basic Energy Science under Contract No. W-7405-Eng-82.

REFERENCES

- [†] Institut für Angewandte Physik, Universität Karlsruhe, 76128 Karlsruhe, Germany.
- [‡] Present address: Department of Physics, Simon Fraser University, Burnaby, BC V5A 16S, Canada.
- ¹ S. Uchida, T. Ido, H. Takagi, T. Arima, Y. Tokura, and S. Tajima, *Phys. Rev. B* **43**, 7942 (1991).
- ² J. P. Falck, A. Levy, M. A. Kastner, and R. J. Birgenau, *Phys. Rev. Lett.* **69**(7), 1109 (1992).
- ³ F. C. Zhang and K. K. Ng, *Phys. Rev. B* **58**(20), 13520 (1998).
- ⁴ Y. Tokura, S. Koshihara, T. Arima, H. Takagi, S. Ishibashi, T. Ido, and S. Uchida, *Phys. Rev. B* **41**, 11657 (1990).
- ⁵ J. Zaanen, G. A. Sawatzky, and J. W. Allen, *Phys. Rev. Lett.* **55**, 418 (1985).
- ⁶ H. S. Choi, Y. S. Lee, T. W. Noh, E. J. Choi, Y. Bang, and Y. J. Kim, *Phys. Rev. B* **60**(7), 4646 (1999).
- ⁷ J. D. Perkins, J. M. Graybeal, M. A. Kastner, R. J. Birgeneau, J. P. Falck, and M. Greven, *Phys. Rev. Lett.* **71**, 1621 (1993).
- ⁸ P. Kuiper, J.-H. Guo, C. Sthe, L.-C. Duda, J. Nordgren, J. J. M. Pothuizen, F. M. F. de Groot, and G. A. Sawatzky, *Phys. Rev. Lett.* **80**, 5204 (1998).
- ⁹ D. Salamon, R. Liu, M. V. K. M. A. Karlow, S. L. Cooper, S. Cheong, W. C. Lee, and D. M. Ginsberg, *Phys. Rev. B* **51**, 6617 (1995).
- ¹⁰ Y. Y. Wang, F. C. Zhang, V. P. Dravid, K. K. Ng, M. V. Klein, S. E. Schnatterly, and L. L. Miller, *Phys. Rev. Lett.* **77**, 1809 (1996).
- ¹¹ L. L. Miller, X. L. Wang, S. X. Wang, C. Stassis, D. C. Johnston, J. Faber, Jr., and

- C. Loong, Phys. Rev. B **41**, 1921 (1990).
- ¹² A. Zibold, H. L. Liu, S. W. Moore, J. M. Graybeal, and D. B. Tanner, Phys. Rev. B **53**(17) (1996).
- ¹³ S. Tajima, T. Ido, S. Ishibashi, T. Itoh, H. Eisaki, Y. Mizuo, T. Arima, H. Takagi, and S. Uchida, Phys. Rev. B **43**, 10496 (1991).
- ¹⁴ M. V. Kurik, Phys. Stat. Sol. A **8**, 8 (1971).
- ¹⁵ The definition of the coupling constant in Ref. 2 is a factor of 1/2 that of the standard convention¹⁹.
- ¹⁶ J. G. Liebler, S. Schmitt-Rink, and H. Haug, J. Lum. **34**, 1 (1985).
- ¹⁷ R. Liu, D. Salamon, M. V. Klein, S. L. Cooper, W. C. Lee, S. Cheong, and D. M. Ginsberg, Phys. Rev. Lett. **71**, 3709 (1993).
- ¹⁸ Y. Toyozawa, *Polarons and Excitons* (Plenum, New York, 1963).
- ¹⁹ G. D. Mahan, *Many-particle physics* (Plenum Pub Corp., 1990), 2nd ed.

FIGURES

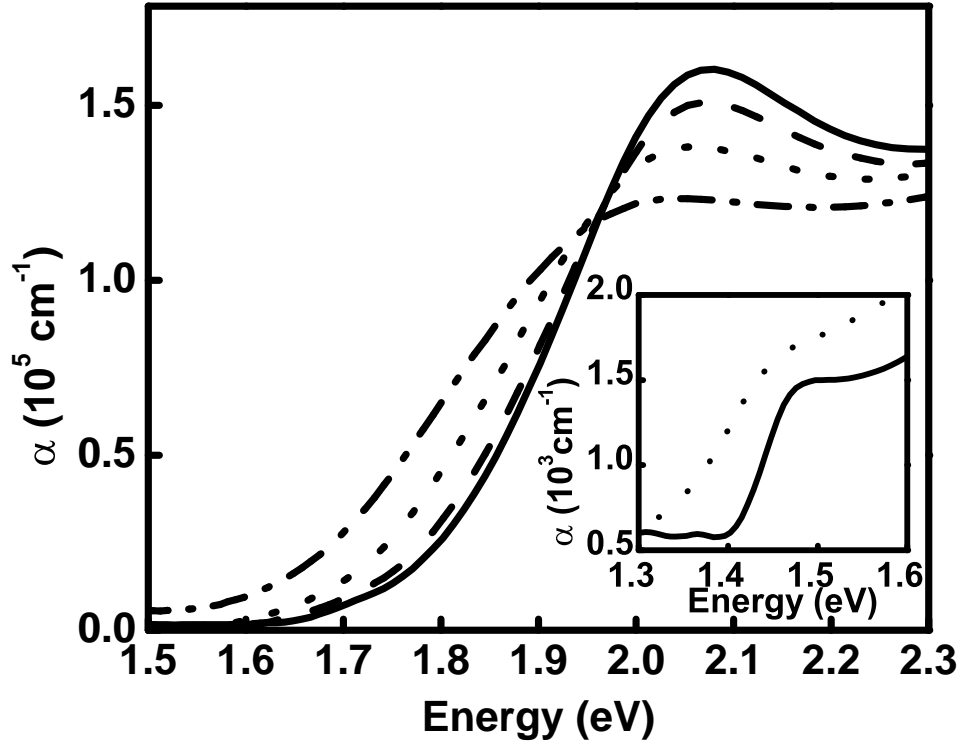


FIG. 1. Absorption coefficient of $\text{Sr}_2\text{CuO}_2\text{Cl}_2$ at different temperature, measured on a $l=950 \text{ \AA}$ thick sample. Inset ($l=300\mu\text{m}$): the weakly allowed d-d transition. Solid lines $T=15 \text{ K}$, dashed line $T=150 \text{ K}$, dotted lines $T=250 \text{ K}$, dashed-dotted line $T=350 \text{ K}$

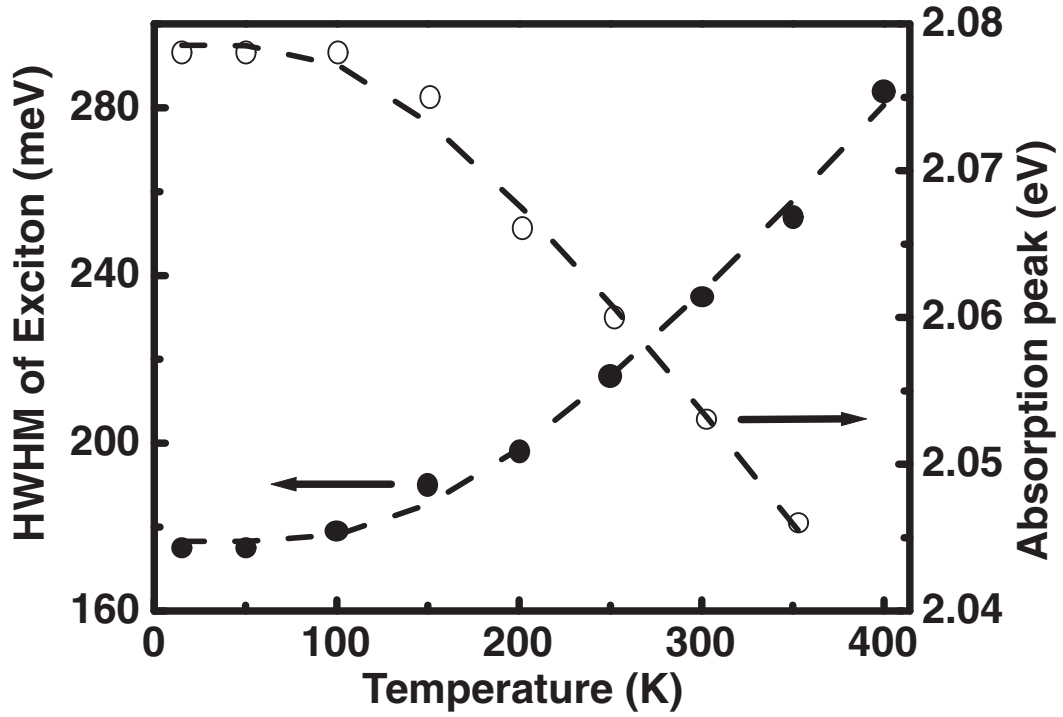


FIG. 2. Half width (solid circles, left axis) and energy (open circles, right axis) of the absorption peak at different temperatures. The dotted shows the best fit to a single oscillator Bose-Einstein occupation function with $E_{boson}=45$ meV

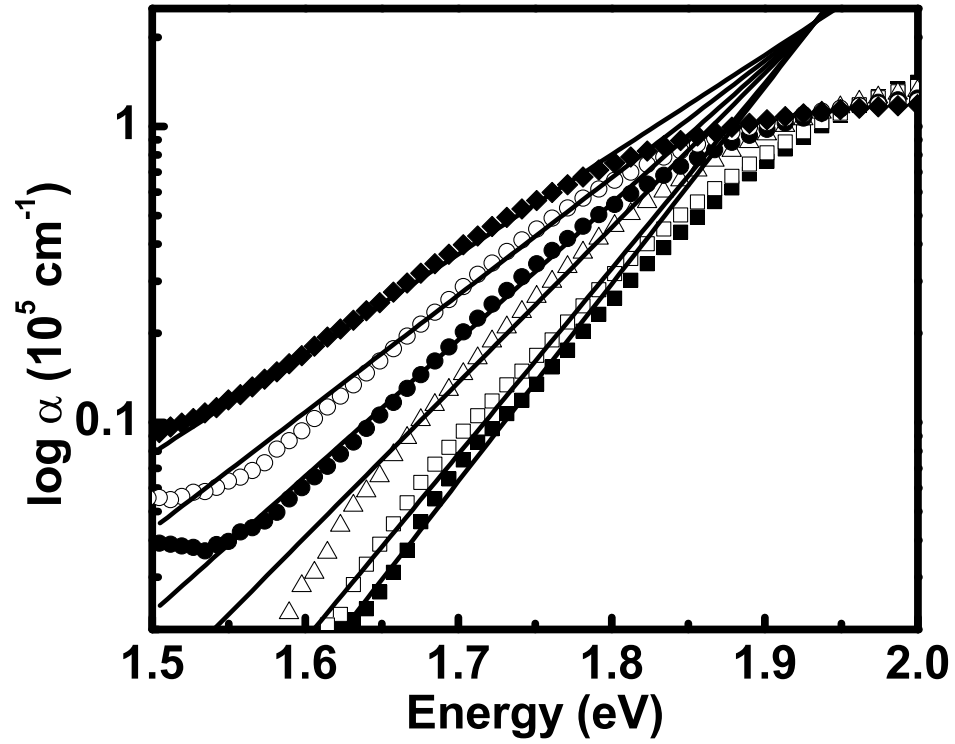


FIG. 3. Logarithmic plot of the absorption coefficient of $\text{Sr}_2\text{CuO}_2\text{Cl}_2$ at selected temperatures, displaying the Urbach-tail. Solid squares $T=15$ K, open squares $T=150$ K, open triangles $T=250$ K, solid circles $T=300$ K, open circles $T=350$ K, diamonds $T=400$ K. The solid lines are fits to the Urbach formula.

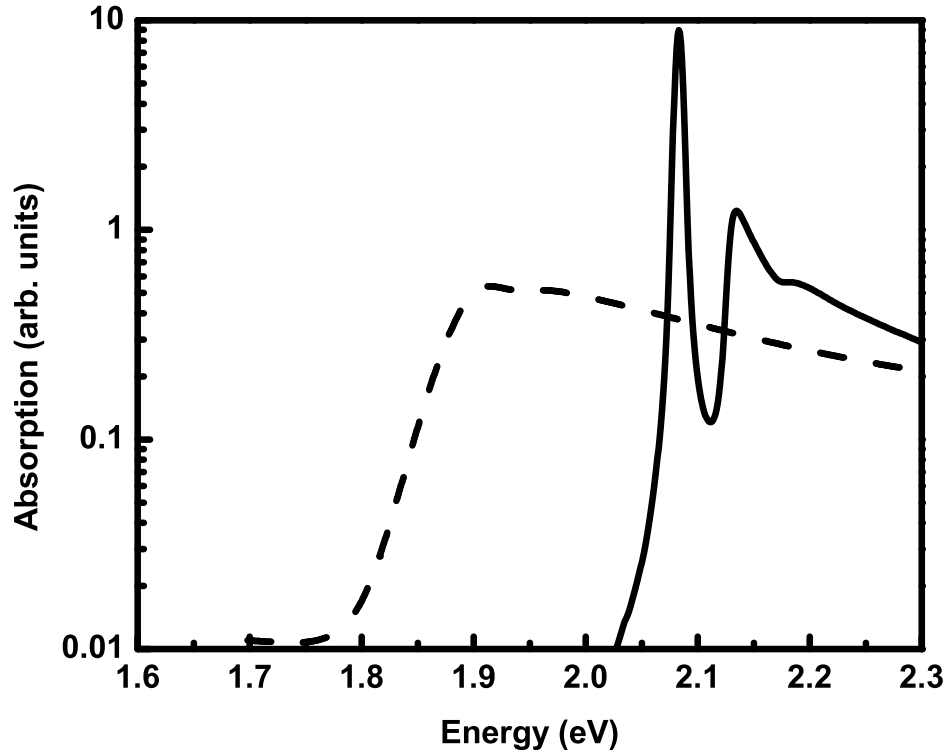


FIG. 4. Absorption coefficient for the excitonic contribution only on a logarithmic scale, calculated for scattering into the exciton and e-h continuum only. Solid line $T=15$ K, dashed line $T=300$ K. The parameters are the same as for the final calculations, except that the coupling constants are twice as big and the inhomogeneous broadening was only 2 meV.

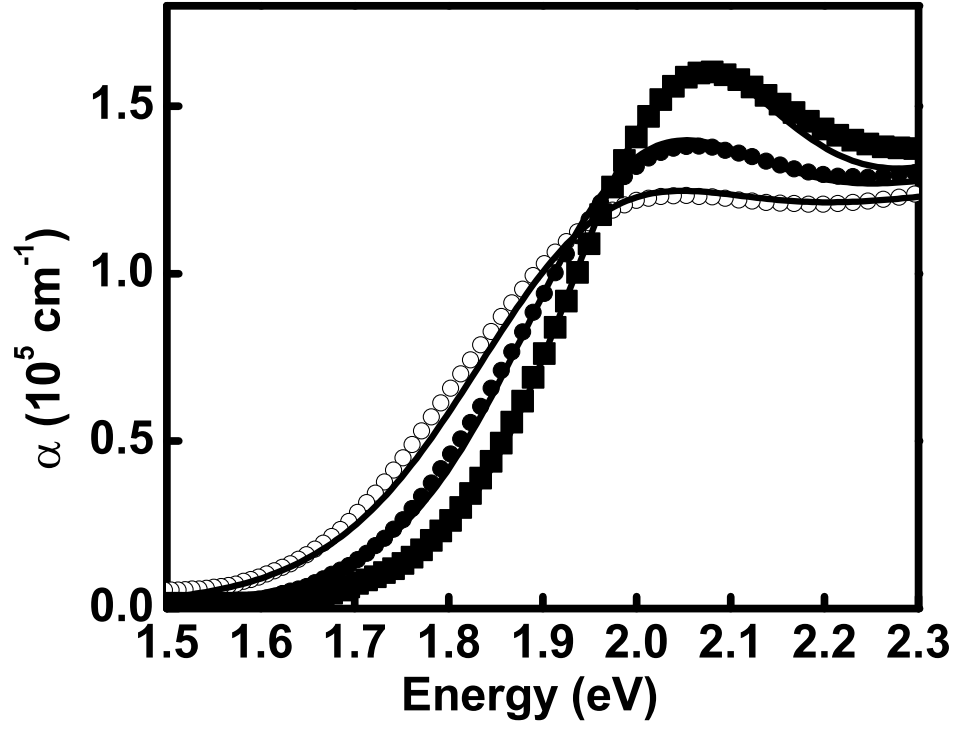


FIG. 5. Absorption coefficient data and theory. Only three temperatures are shown for clarity. Squares $T=15$ K, closed circles $T=250$ K, open circles $T=350$ K, solid lines are the theoretical results.

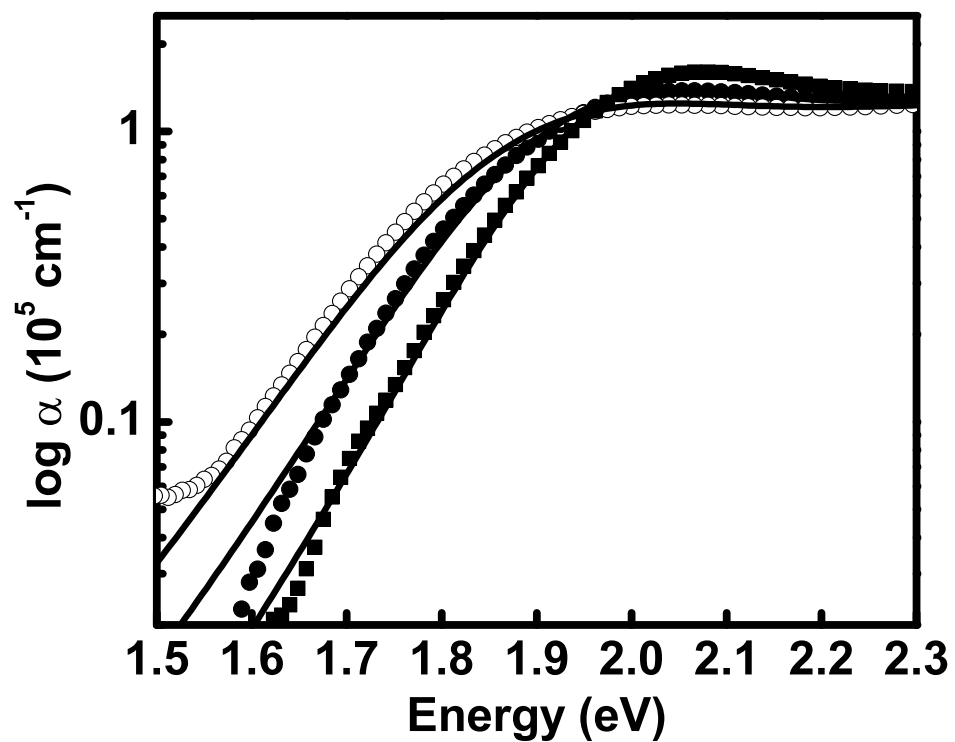


FIG. 6. Absorption coefficient data and theory, displayed on a semi-logarithmic scale. Only three temperatures are shown for clarity. Squares $T=15$ K, closed circles $T=250$ K, open circles $T=350$ K, solid lines are the theoretical results.